

# Ballistic Impact Response of Multi-Layers Armors Against Piercing Projectile: Finite Element Modeling



Hassouna Amira and Salah Mezlini

**Abstract** The development of reliable bulletproof vests requires the study of the factors that affect the ballistic resistance of the body armor. The numerical simulation is a fundamental tool adopted in this process. This work is focused on the ballistic performance of a multi-layer armor against an ogival nosed hardened steel projectile. The multi-layers armors are constituted of two composite layers and a ceramic layer. The Johnson-Holmquist-2 (JH-2) model was employed for modeling the behavior and damage of ceramic material and the Hashin criterion for simulating the damage of the composite material. The projectile was considered as a deformable part and its behavior is governed by the Johnson–Cook (JC) model. The results reveal that the residual velocity is highly influenced by the impact velocity. The effectiveness of the body armor is reduced by increasing the impact velocity. Furthermore, it is found that adding a thin composite layer in front of the ceramic layer can reduce the damage of the back layer made of composite material. The ballistic resistance is improved by increasing the thickness of both ceramic and composite plates. The residual velocity is more influenced by the thickness of the ceramic plate than by the thickness of the composite plate.

**Keywords** Ballistic performance · Body armors · Ceramic and composite thicknesses

## 1 Introduction

The development of high-performance bulletproof vests with a high level of protection is a great challenge for researchers and manufacturers. To contribute to this development, it is necessary to study and better understand the effects induced by the ballistic impact of a projectile against ceramic armor [1, 2], composite armor [3,

---

H. Amira (✉) · S. Mezlini

Laboratoire de Génie Mécanique, Ecole Nationale d'Ingénieurs de Monastir, Université de Monastir, Monastir, Tunisia

e-mail: [Hassounaamira0@gmail.com](mailto:Hassounaamira0@gmail.com)

4] and bilayers armors consisting of ceramic and composite plates [5]. Based on Artificial Neural Networks, Malik et al. [6] evaluated the absorbed energy of composite laminate subjected to low velocity when the thickness, the stacking sequence, and the number of layers are varied. The ballistic performance of the composite increases with the thickness and the number of laminate layers. Khan et al. [1] performed an experimental and numerical study to explore the ballistic resistance of a ceramic target against ogival nosed projectile. It was found that the absorbed energy decreases with the increase of the impact velocity. Moreover, the damage in the target increases with the angle of obliquity. Feli et al. [7] analyzed the ballistic perforation of ceramic composite armors against cylindrical tungsten projectiles. The results show that the delamination of composite layers and the angle of the ceramic cone decrease with increasing the impact velocity.

Motivated by the previously mentioned research, a new design of body armor was developed. This body armor was composed of two layers of composite materials and a ceramic layer inserted in the middle. The objective of this work is to study the ballistic resistance of multiple layer armor under single hit using finite element method. Furthermore, the effect of design parameters (ceramic and composite thicknesses) as well as the effect of the impact velocity on the ballistic performance (residual velocity and target damage) were examined.

## 2 Finite Element Modeling

### 2.1 Description of the Finite Element Model

To simulate the ballistic impact of ceramic and composite materials against ogival nosed projectile, a Finite Element (FE) model is developed through the Abaqus / explicit code. Figure 1 shows a description of the finite element model and meshing. The target is composed of three layers, two composite layers, and a ceramic plate inserted in the middle of these two layers. The thickness of the forward composite layer, the ceramic layer, and the back composite layer are 1.5 mm, 5 mm, and 3 mm, respectively. The dimension of the target is  $120 \times 120 \times 9,5 \text{ mm}^3$ . The projectile is in hard steel, with a diameter of 7.62 mm and a mass of 30 g. The lateral sides of the target are embedded, and an impact velocity of 275 m/s is applied to the impactor, which is assumed to be deformable. The ceramic layer and the projectile are meshed with C3D8R three-dimensional elements, while the composite layer is meshed with SC8R elements. A general contact algorithm is adopted between the projectile and the target and between the target layers. The coefficient of friction between the projectile/ ceramic plate and the projectile/ composite plate is assumed to be negligible; this assumption was adopted based on the high impact speed.

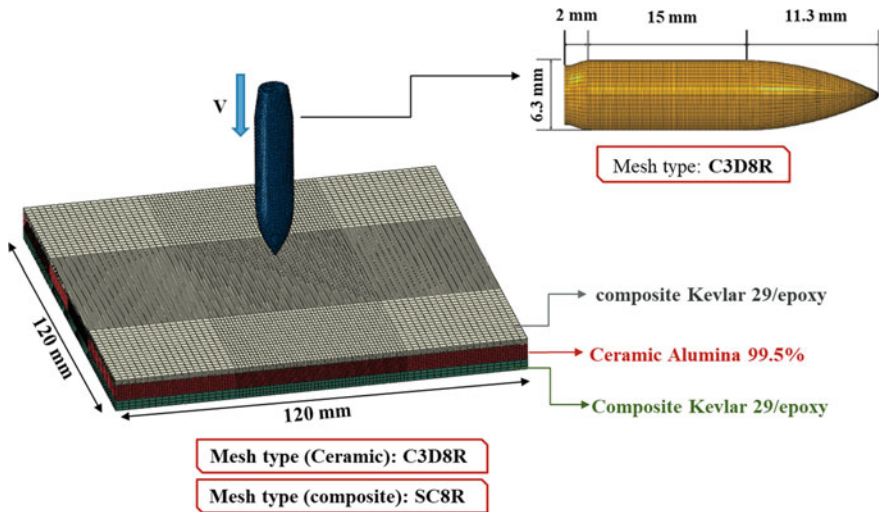


**Fig. 1** Description of the finite element model and meshing

## 2.2 Material Properties

In this study, two behavior laws are used for modeling the target material. The composite Kevlar/ epoxy is modeled as an anisotropic material, and the Hashin criterion is adopted to describe the damage initiation and evolution of this material. The Johnson-Holmquist model [Holmquist et al. 1993] (JH-2) is employed to describe the behavior and the damage of the ceramic plate. The material parameters are summarized in the following tables (Tables 1 and 2). The Johnson–Cook (JC) behavior law and failure model are applied to the projectile, which is made of steel 4340. The Johnson cook parameters are illustrated in the Table 3.

**Table 1** Properties of Kevlar/epoxy [8]

$E_1$ (GPa)	$E_2$ (GPa)	$E_3$ (GPa)	$\nu_{12}$	$\nu_{13}$	$\nu_{23}$
25.63	25.63	7.5	0.2	0.3	0.3
$G_{12}$ (GPa)	$G_{13}$ (GPa)	$G_{23}$ (GPa)	$X^T$ (MPa)	$X^C$ (MPa)	$Y^T$ (MPa)
2.12	5.43	5.43	586	112	586
$Y^C$ (MPa)	$S^L$ (MPa)	$S^T$ (MPa)	$\rho$ (Kg/m <sup>3</sup> )		
112	66	66	1251		

**Table 2** Properties of Ceramic (Alumin 99%) [8]

G (GPa)	HEL (GPa)	A	N	C	$\rho$ (Kg/m <sup>3</sup> )
90.16	19	0.93	0.6	0	3890
<b>B</b>	<b>M</b>	$\sigma_{fmax}$	<b>PHEL (GPa)</b>	<b>D<sub>1</sub></b>	<b>D<sub>2</sub></b>
0.31	0.6	0.2	1.46	0.005	1
$\beta$	<b>K<sub>1</sub> (GPa)</b>	<b>K<sub>2</sub> (GPa)</b>	<b>K<sub>3</sub> (GPa)</b>		
1	130.95	0	0		

**Table 3** Properties of projectile material (steel 4340) [8]

E (GPa)	$\nu$	$\rho$ (Kg/m <sup>3</sup> )	A (GPa)	B (GPa)	n
210	0.3	7850	0 0.95	0 0.725	0.375
<b>C</b>	<b>m</b>	<b>D1</b>	<b>D2</b>	<b>D3</b>	<b>D4</b>
0.015	0.625	-0.8	2.1	0.5	0.002
<b>D5</b>	<b>T<sub>f</sub> (K)</b>	<b>T<sub>a</sub> (K)</b>	$\epsilon^{-0}_p$ (s <sup>-1</sup> )		
0.61	1793	293	1		

### 3 Results and Discussion

#### 3.1 Validation of the Finite Element

The validation of the finite element model is carried out for each component of the target, independently. Firstly, the composite model is validated by the trials performed by Millan et al. [4] (Table 4). Secondly, the results' issues from the ceramic model are validated by those obtained by Khan et al. [1] (Fig. 2). The FE model made of a composite plate is vetted by comparing the residual velocity of the numerical model to the experimental one from the literature. Moreover, the FE model of the ceramic is validated in terms of damage on the backside of the target. It can be noticed that a strong fit is obtained between our numerical results and the results of the literature for both models. Both numerical and experimental results show that radial cracks form on the back surface of the ceramic plate.

**Table 4** Comparison between our numerical results and the results of the literature

Our numerical model	Impact velocity = 300 m/s	Residual velocity = 243 m/s
Literature [4]	Impact velocity = 300 m/s	Residual velocity = 245 m/s

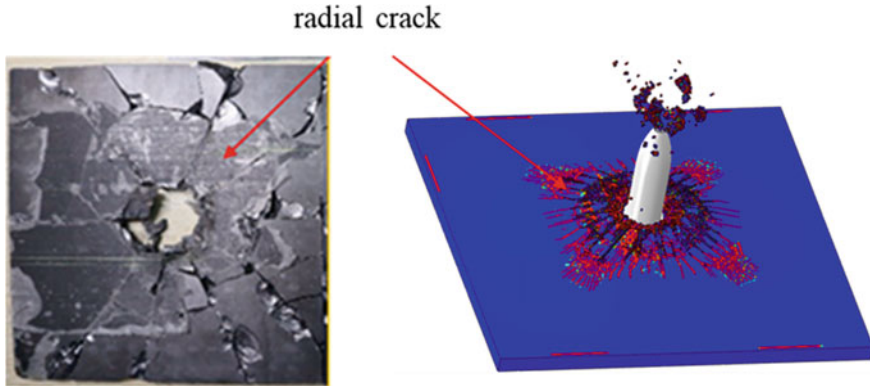
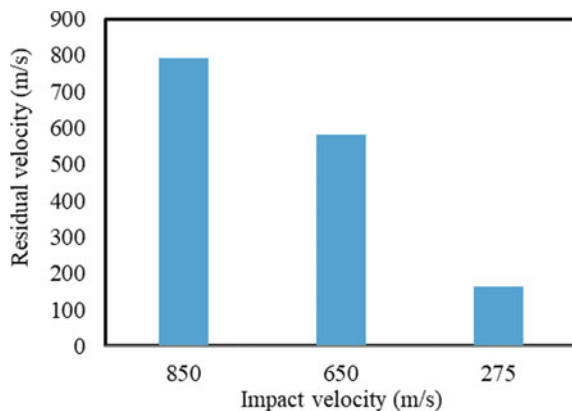


**Fig. 2** Comparison of numerical and experimental ceramic failure modes

### 3.2 *Effect of Impact Velocity*

To highlight the effect of the impact velocity on the residual velocity, three impact velocities 275, 650, and 850 m/s were tested. Figure 3 shows the evolution of the residual velocity versus the impact velocity. It can be noted that the residual velocity is highly influenced by the impact velocity. The increase in the impact velocity results in a decrease in the average relative difference between the impact velocity and the residual velocity. For an impact speed of 275 m/s, the observed residual velocity is 164 m/s, i.e., an average relative error of 40%. For an impact velocity of 850 m/s, the residual velocity is 792 m/s, so the average relative error is 6%. It can be concluded that the performance of the body armor, meaning the energy absorbed, decreases as the impact velocity increases.

**Fig. 3** Effect of the impact velocity on the residual velocity



### 3.3 Comparison Between Two- and Three-Layer Targets

Figure 4 illustrates the damage distribution in the ceramic plate and composite back layer for bilayer target and three-layer target. It is noted that the damage to the composite part for the bilayer target is more pronounced than that of the tri-layer target. In fact, for the three-layer target, the absorbed energy is spread over three layers instead of two, minimizing the damage to the rear composite layer. It is observed that the fracture in the composite plate is oriented toward the transverse direction of the fiber, which is explained by the low strength of the matrix compared to that of the fiber. Concerning the damage of the ceramic plate, it can be seen that radial cracks form in the ceramic plate, and these are more important in the three-layer target than in the two-layer target. This result is explained by the deflection of the composite plate in front of the ceramic plate, which provides the propagation of cracks in the ceramic plate.

To examine the effect of adding a composite layer in front of the ceramic layer, a comparison between bilayer target formed with ceramic layer and composite backing layer and three-layer target, in which the ceramic is inserted in the middle of two composite layers, is shown in Fig. 5. It is found that the addition of a composite layer in front of the ceramic plate has a negligible influence on the residual velocity. This can be explained by the small thickness of the added composite layer. Therefore, the objective of the following section is to investigate the effect of the composite and ceramic thicknesses on the residual velocity.

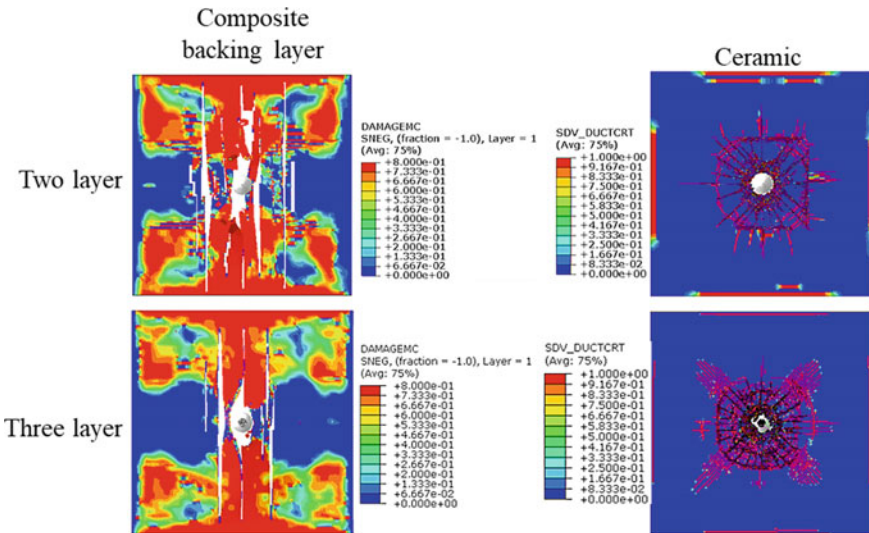
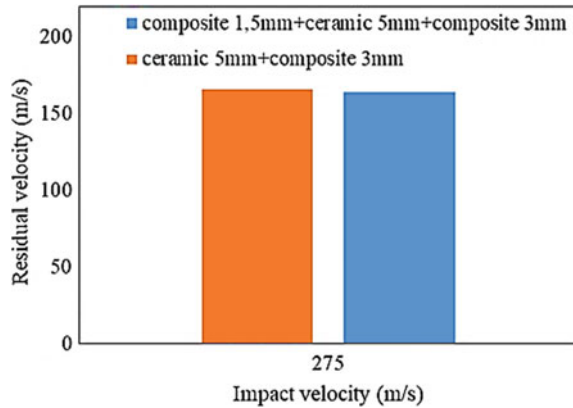


Fig. 4 Comparison of damage between two- and three-layer targets

**Fig. 5** Comparison of residual velocity between two- and three-layer targets



### 3.4 Effect of the Design Parameters

To evaluate the effect of composite and ceramic thicknesses on the residual velocity, different tests were performed (Table 5). Figure 6 illustrates the evolution of residual velocity as a function of composite and ceramic plate thicknesses. It can be seen that increasing the thickness of the back composite layer (from test 1 to test 2) and the front composite layer (from test 2 to test 3) has a little influence on the residual velocity. Indeed, increasing the thickness of the composite from 3 to 5 mm generates a decrease in the residual velocity from 164 to 156 m/s, resulting in an average relative difference of 4%. Moreover, when the composite thickness passes from 3 to 10 mm (from test 3 to test 4), an average relative error of 16% is detected. This proves that the thickness of the composite has an influence on the residual velocity, if it undergoes a very large variation. The effect of the ceramic thickness on the residual velocity is observed in tests 5 and 6. We can see that when the ceramic thickness increases from 5 to 8 mm, the residual velocity decreases of about 65% and the impactor is totally penetrated. However, when the ceramic thickness reaches 10 mm, the impactor is completely blocked, and the kinetic energy of the projectile is totally absorbed by the target. It can be inferred that the ceramic thickness has a great influence on the ballistic resistance.

Figure 7 shows the target penetration depth (pd) for different ceramic and composite thicknesses. It is observed that the ceramic and composite thicknesses have a significant influence on the target deformation. When the composite plate thickness varies (from test 2 to test 3), the depth of penetration varies from 20 to 11.9 mm. A decrease of about 40% was detected. As the thickness of the ceramic plate increases (Trial 3 to Trial 5), the depth of penetration decreases from 11.9 to 2.6 mm. A decrease of about 78% was observed. It can be deduced that increasing the thickness of the composite and ceramic plates leads to a decrease in the target deformation. The low penetration depth is observed for high ceramic thickness.

**Table 5** Performed tests

Tests	Composite front layer (mm)	Ceramic plate (mm)	Composite back layer (mm)
Test 1	1.5	5	3
Test 2	3	5	3
Test 3	3	5	5
Test 4	10	5	5
Test 5	3	8	5
Test 6	3	10	5

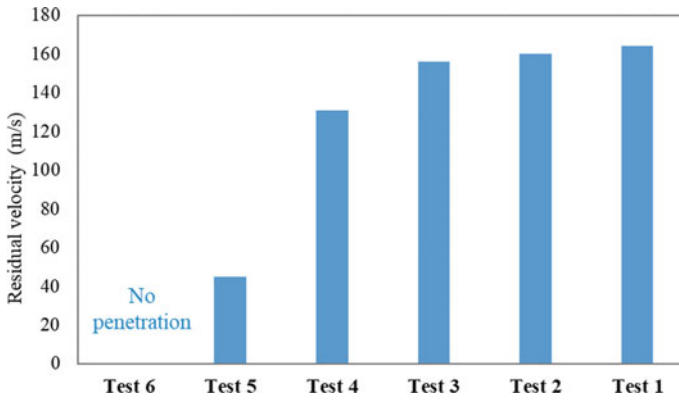


**Fig. 6** Effect of the composite and ceramic thicknesses on the residual velocity



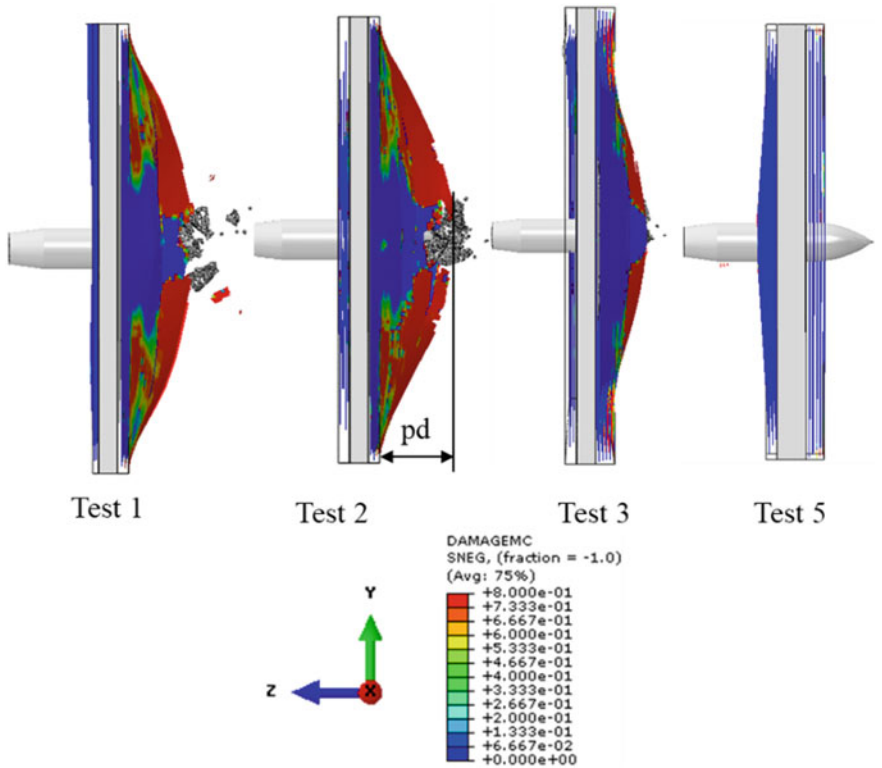


Fig. 7 Effect of composite and ceramic thicknesses on the depth of penetration

## 4 Conclusion

This paper studied the ballistic performance of multiple layer armor formed with two composite layers and one ceramic layer inserted in the middle against ogival nosed projectile. The influence of the impact velocity as well as the influence of ceramic and composite thicknesses on the residual velocity and the target damage are examined using numerical simulation. It was found that the ballistic performance of body armor decreases with increasing the impact velocity. In addition, ceramic and composite thicknesses have a considerable influence on the residual velocity. The residual velocity is more affected by the ceramic thickness than the composite thickness. The target deformation decreases with increasing both ceramic and composite thicknesses.

The perspectives envisaged in this study are the investigation of the effects of the projectile obliquity angle and its diameter on the ballistic performance of the bulletproof vest.

**Acknowledgements** I would like to thank the Applied Mechanics and Engineering laboratory (LMAI) of the National Engineering School of Tunis for the Abaqus license.

## References

1. M. K. Khan, M. A. Iqbal, V. Bratov, N. F. Morozov, and N. K. Gupta, "An investigation of the ballistic performance of independent ceramic target," *Thin-Walled Structures*, vol. 154, no. January, p. 106784, 2020, doi: <https://doi.org/10.1016/j.tws.2020.106784>.
2. R. Zaera and V. Sánchez-Gálvez, "Modelling of fracture processes in the ballistic impact on ceramic armours," *Journal De Physique.*, vol. 7, no. 3, 1997, doi: <https://doi.org/10.1051/jp4:19973117>.
3. G. Gopinath, J. Q. Zheng, and R. C. Batra, "Effect of matrix on ballistic performance of soft body armor," *Compos Struct*, vol. 94, no. 9, pp. 2690–2696, Sep. 2012. <https://doi.org/10.1016/j.compstruct.2012.03.038>
4. M. Rodríguez Millán, C. E. Moreno, M. Marco, C. Santiuste, and H. Miguélez, "Numerical analysis of the ballistic behaviour of Kevlar® composite under impact of double-nosed stepped cylindrical projectiles," *Journal of Reinforced Plastics and Composites*, vol. 35, no. 2, pp. 124–137, Jan. 2016, doi: <https://doi.org/10.1177/0731684415608004>.
5. Z. Fawaz, W. Zheng, and K. Behdinan, "Numerical simulation of normal and oblique ballistic impact on ceramic composite armours," *Compos Struct*, vol. 63, no. 3–4, pp. 387–395, 2004. [https://doi.org/10.1016/S0263-8223\(03\)00187-9](https://doi.org/10.1016/S0263-8223(03)00187-9)
6. M. H. Malik and A. F. M. Arif, "ANN prediction model for composite plates against low velocity impact loads using finite element analysis," *Compos Struct*, vol. 101, pp. 290–300, Jul. 2013. <https://doi.org/10.1016/j.compstruct.2013.02.020>
7. S. Feli and M. R. Asgari, "Finite element simulation of ceramic/composite armor under ballistic impact," *Compos B Eng*, vol. 42, no. 4, pp. 771–780, Jun. 2011. <https://doi.org/10.1016/j.compositesb.2011.01.024>
8. G. Guo, S. Alam, and L. D. Peel, "Numerical analysis of ballistic impact performance of two ceramic-based armor structures," *Composites Part C: Open Access*, vol. 3, no. October, p. 100061, 2020, doi: <https://doi.org/10.1016/j.jcomc.2020.100061>.